BIOCHEMISTRY

A matricellular protein fibulin-4 is essential for the activation of lysyl oxidase

Kazuo Noda[1,2]*, Kaori Kitagawa[1]*, Takao Miki[1], Masahito Horiguchi[3], Tomoya O. Akama[1], Takako Taniguchi[4], Hisaaki Taniguchi[4], Kazuaki Takahashi[5], Yasumitsu Ogra[5], Robert P. Mecham[6], Masahiko Terajima[7], Mitsuo Yamauchi[7], Tomoyuki Nakamura[1†]

Fibulin-4 is a matricellular protein required for extracellular matrix (ECM) assembly. Mice deficient in fibulin-4 (*Fbln4*$^{-/-}$) have disrupted collagen and elastin fibers and die shortly after birth from aortic and diaphragmatic rupture. The function of fibulin-4 in ECM assembly, however, remains elusive. Here, we show that fibulin-4 is required for the activity of lysyl oxidase (LOX), a copper-containing enzyme that catalyzes the covalent cross-linking of elastin and collagen. LOX produced by *Fbln4*$^{-/-}$ cells had lower activity than LOX produced by wild-type cells due to the absence of lysine tyrosyl quinone (LTQ), a unique cofactor required for LOX activity. Our studies showed that fibulin-4 is required for copper ion transfer from the copper transporter ATP7A to LOX in the trans-Golgi network (TGN), which is a necessary step for LTQ formation. These results uncover a pivotal role for fibulin-4 in the activation of LOX and, hence, in ECM assembly.

INTRODUCTION

Elastic fibers and collagen fibers are the major extracellular matrices (ECMs) that confer resilience and tensile strength on tissues, respectively. Elastic fibers are assembled from elastin protein aggregates deposited onto microfibrils (*1*), and collagen fibers consist of bundles of collagen fibrils that are formed by the self-assembly of triple-helical collagen molecules (*2*). Both elastin and collagen fibers undergo extensive lysine-derived cross-linking outside the cell to form the stable polymers that define their functional forms. Although elastin and collagens do not share similar sequences, the cross-linking of both proteins is initiated by the same enzyme, lysyl oxidase (LOX) (*3*, *4*).

LOX is a member of a copper amine oxidase family that includes LOX and LOX-like (LOXL) 1 to 4. LOX family members contain a highly conserved catalytic domain with a lysine tyrosyl quinone (LTQ) redox cofactor and a conserved copper-binding site in the C-terminal half of the protein (*5*, *6*). The N-terminal domains are variable in length and sequence, and those of LOX and LOXL1 function as propeptides, as they are proteolytically cleaved to release active enzyme (*7*). The propeptides are considered to function in secretion and distribution of the enzymes, suppression of the enzyme activity until proteolytically removed, or modulation of cell signaling (*8*, *9*). LOXL2 to LOXL4 comprise a subfamily whose N-terminal domains contain scavenger receptor cysteine-rich domains, the function of which is not well understood (*8*). Mice deficient in LOX (*Lox*$^{-/-}$) show defective cross-linking of elastin and collagen that leads to severe aortic aneurysm and emphysematous lungs and die perinatally due to aortic and diaphragmatic rupture (*10*, *11*). In contrast, mice deficient in either of LOXL1 to LOXL3 survive to adulthood and show much less severe phenotypes than *Lox*$^{-/-}$ mice (*12*–*14*). Mice deficient in LOXL4 have not been reported. Therefore, LOX is considered to be the enzyme that plays a major role in cross-linking elastin and collagen, at least in the developmental stage.

The LOX enzyme is activated extracellularly when the propeptide is proteolytically removed from the proenzyme (proLOX) by the proteases bone morphogenetic protein 1 (BMP-1) or mammalian Tolloid-like 1 (mTLL-1), resulting in release of the catalytically active mature LOX (fig. S1, A and C) (*15*). Both copper binding and LTQ formation, which occur in the trans-Golgi network (TGN), are required for full enzyme activity. Copper binding to key histidine residues in LOX facilitates the formation of LTQ, an intramolecular cross-link between Lys^{314} and Tyr^{349} side chains (in the case of murine LOX) (fig. S1B) (*5*).

The fibulins are a family of matricellular proteins that function in the ECM but do not play a structural role (*16*). Fibulin-4, along with its closely related paralog fibulin-5, plays an essential role in elastogenesis. Mice deficient in fibulin-5 (*Fbln5*$^{-/-}$) survive to adulthood, but exhibit severe emphysema, stiff and tortuous arteries, and loose skin, due to defective elastogenesis (*17*, *18*). Collagen fibers are not affected, and aneurysms are not found in these mice. Mice deficient in fibulin-4 (*Fbln4*$^{-/-}$), in contrast, show phenotypes that closely overlap with those of *Lox*$^{-/-}$ mice, including perinatal lethality due to aortic and diaphragmatic rupture, severe aortic aneurysms, and emphysematous lungs, with severely disrupted elastic fibers and abnormal collagen fibers (*19*, *20*). These phenotypic similarities suggest a functional link between fibulin-4 and LOX. Our previous data showed that the LOX propeptide interacts with fibulin-4, but not with fibulin-5 (*17*, *21*). However, whether fibulin-4 is necessary for LOX activity has been elusive.

To elucidate whether and how fibulin-4 influences LOX activity, we explored the nature of LOX produced in the absence of fibulin-4. Here, we report that LOX secreted from *Fbln4*$^{-/-}$ cells is inactive due to the inability of LOX to form the LTQ cofactor. We show that fibulin-4 is required for copper ion transfer from the copper transporter ATP7A to proLOX in the lumen of TGN. We also report that

[1]Department of Pharmacology, Kansai Medical University, Hirakata, Osaka 573-1010, Japan. [2]Department of Plastic and Reconstructive Surgery, Graduate School of Medicine, Kyoto University, Kyoto 606-8507, Japan. [3]Department of Emergency Medicine, Japanese Red Cross Society Kyoto Daiichi Hospital, Kyoto 605-0981, Japan. [4]Division of Disease Proteomics, Institute for Enzyme Research, Tokushima University, Tokushima 770-8503, Japan. [5]Laboratory of Toxicology and Environmental Health, Graduate School of Pharmaceutical Sciences, Chiba University, Chiba 260-8675, Japan. [6]Department of Cell Biology and Physiology, Washington University School of Medicine, Saint Louis, MO 63110, USA. [7]Division of Oral and Craniofacial Health Sciences, Adams School of Dentistry, University of North Carolina, Chapel Hill, NC 27599, USA.
*These authors contributed equally to this work.
†Corresponding author. Email: nakamtom@hirakata.kmu.ac.jp

secreted fibulin-4 can be internalized by endocytosis and contribute to the activation of LOX in the TGN. These results establish a pivotal role for fibulin-4 as an indispensable partner of LOX for its enzymatic activity.

RESULTS

The N-terminal domain of fibulin-4 is required for interaction with proLOX

A homozygous N-terminal missense mutation in the human *FBLN4* gene (E57K) was reported to cause cutis laxa syndrome, with ascending aortic aneurysms, arterial tortuosity, emphysema, and joint laxity (*22*). Because we previously showed that fibulin-4 interacts with the propeptide domain of proLOX (*21*), we examined whether the interaction between the two proteins is affected by mutation or truncation within the N-terminal region of fibulin-4. We used an in vitro binding assay using fibulin-4 mutants and proLOX overexpressed by 293T engineered by CRISPR-Cas9–based gene targeting to inactivate BMP-1 and avoid propeptide cleavage. The results confirmed that the interaction between the two proteins is largely dependent on the N-terminal domain of fibulin-4, as proLOX did not coprecipitate with N-terminal fibulin-4 deletion mutants (ΔN1 and ΔN2). Similarly, the E57K mutant of fibulin-4 reacted only weakly with proLOX (Fig. 1).

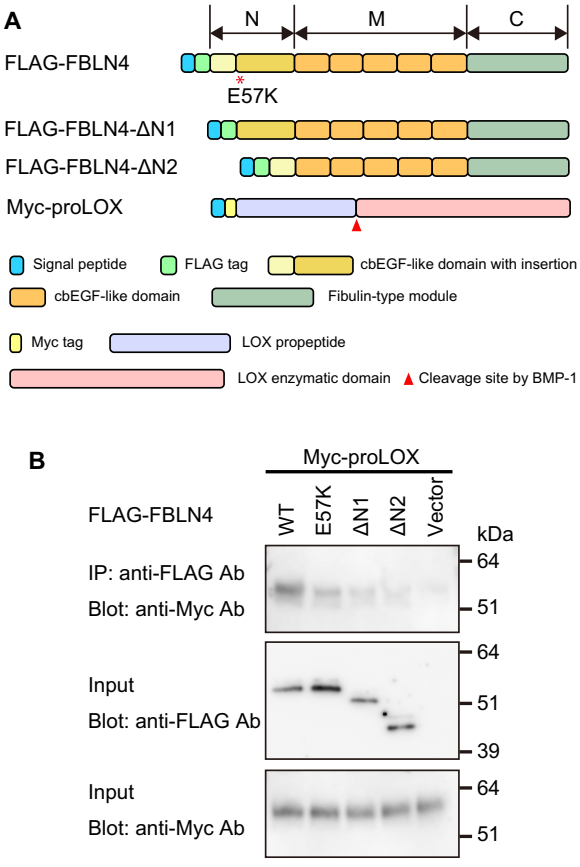

Fig. 1. An in vitro binding assay showing a domain-specific binding of fibulin-4 (FBLN4) with proLOX. (**A**) Domain structure of FLAG-tagged full-length fibulin-4 and fibulin-4 mutants (E57K, ΔN1, and ΔN2) and Myc-tagged proLOX used in the assay. (**B**) In vitro binding assay using the conditioned medium from 293T (*BMP1*$^{-/-}$) cells transfected with plasmids encoding the cDNAs shown in (A). The lysates were mixed and immunoprecipitated with anti-FLAG agarose beads, followed by SDS-PAGE and Western blotting using anti-Myc and anti-FLAG antibodies (Ab). Note strong binding of proLOX with WT fibulin-4, while the binding was much weaker with E57K mutant fibulin-4 and even weaker with N-terminal deletion mutants.

LOX produced in the absence of fibulin-4 has altered posttranslational modification

To examine whether loss of fibulin-4 affects LOX protein in vivo, we performed Western blot analyses with an anti-LOX antibody of mouse neonatal aortic tissue extract. We detected only mature LOX enzyme without the propeptide; no proLOX was detectable in these tissues. Levels of mature LOX in *Fbln4*$^{-/-}$ tissues were comparable to those in wild-type (WT) aorta (Fig. 2A). However, mature LOX from *Fbln4*$^{-/-}$ aortic tissues, but not from *Fbln5*$^{-/-}$ aortic tissues, migrated slightly slower in SDS–polyacrylamide gel electrophoresis (SDS-PAGE) than LOX from WT aortic tissues (Fig. 2A).

This mobility shift was also evident in cell culture experiments where endogenously expressed LOX secreted into the culture medium of *Fbln4*$^{-/-}$ mouse embryonic fibroblasts (MEFs) migrated in SDS-PAGE slower than that from WT MEFs (Fig. 2, B and C). Lentiviral expression of full-length WT fibulin-4 in *Fbln4*$^{-/-}$ MEFs reversed the mobility shift, with secreted LOX running at a size equivalent to the WT protein. Lentiviral expression of fibulin-4 with the E57K mutation only partially rescued the mobility shift of LOX, and no rescue was observed with N-terminal deletion mutant of fibulin-4 or full-length fibulin-5 (Fig. 2, B and C). LOX-FLAG secreted from *Fbln4*$^{-/-}$ MEFs infected with a lentivirus expressing C-terminally FLAG-tagged proLOX complementary DNA (cDNA) also exhibited delayed migration, indicating that the mobility shift was caused by altered posttranslational modification and not by alternative splicing (Fig. 2, D and E).

Fibulin-4 is necessary for LOX enzymatic activity

To explore the functional differences between the two forms of LOX, we purified endogenously expressed LOX from the conditioned medium of WT and *Fbln4*$^{-/-}$ MEFs (Fig. 3A) and measured LOX enzymatic activity using tritiated tropoelastin as a substrate. LOX from *Fbln4*$^{-/-}$ MEFs was substantially less active than an equivalent amount of WT LOX (Fig. 3B). Consistent with this finding, levels of desmosine and isodesmosine, LOX-derived cross-links in elastin, and pyridinoline, a cross-link in collagen, were greatly reduced in neonatal aortae of both *Fbln4*$^{-/-}$ and *Lox*$^{-/-}$ mice compared to WT neonatal mouse aortae (Fig. 3, C and D). These results indicate that fibulin-4 is essential for the full enzymatic activity of LOX in vitro and in vivo.

Fibulin-4 is necessary for LTQ formation in LOX

There are four known posttranslational modifications of proLOX: glycosylation of the propeptide (*23*), cleavage of the propeptide (*24*), sulfation of tyrosine residues in LOX enzyme domain (*25*), and LTQ formation after copper ion binding (*5*). Because all potential glycosylation sites are within the propeptide (*23*), this modification cannot cause the mobility shift of mature LOX enzyme after cleavage of the propeptide. We then examined whether the cleavage site of proLOX differs between WT and *Fbln4*$^{-/-}$ cells. The N-terminal sequences of mature LOX purified from the conditioned medium of WT and *Fbln4*$^{-/-}$ MEFs were analyzed by Edman degradation. There was no difference in amino acid sequence between the genotypes, indicating that the mobility shift of LOX produced by *Fbln4*$^{-/-}$ cells

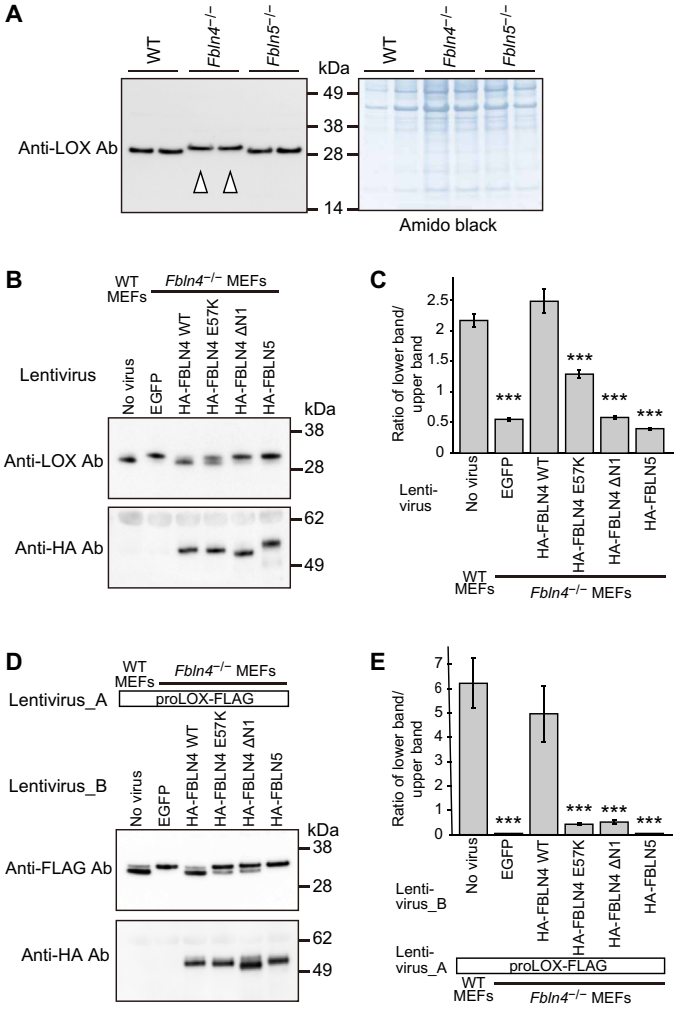

Fig. 2. Mobility shift of LOX produced in the absence of fibulin-4 in SDS-PAGE. (**A**) Western blot analysis with anti-LOX antibody (left) and amido black staining of the same membrane (right) of mouse neonatal aortic tissue lysate (a pup/lane) of the indicated genotype. Note that LOX from *Fbln4*$^{-/-}$ aortic tissues migrated slightly slower than that from WT and *Fbln5*$^{-/-}$ tissues (open arrowheads). (**B**) Western blot analysis of LOX endogenously expressed by WT and *Fbln4*$^{-/-}$ MEFs. Note the distinct effects of lentiviral overexpression of HA-tagged fibulin-4 (HA-FBLN4 WT), E57K mutant fibulin-4 (HA-FBLN4 E57K), N-terminally deleted fibulin-4 (HA-FBLN4 ΔN1), and full-length fibulin-5 (HA-FBLN5) on LOX migration. (**C**) Ratio of the quantified intensity of lower and upper bands of LOX. (**D**) Western blot analysis of overexpressed LOX by infecting WT and *Fbln4*$^{-/-}$ MEFs with C-terminally FLAG-tagged proLOX (proLOX-FLAG) lentivirus. Note the mobility shift of LOX-FLAG secreted by *Fbln4*$^{-/-}$ MEFs and distinct effects of lentiviral overexpression of HA-FBLN4 WT, HA-FBLN4E57K, HA-FBLN4 ΔN1, and HA-FBLN5 on LOX-FLAG migration. (**E**) Ratio of the quantified intensity of lower and upper bands of LOX-FLAG. Bar graphs show mean ± SEM ($n = 4$). ***$P < 0.001$ compared with WT MEFs.

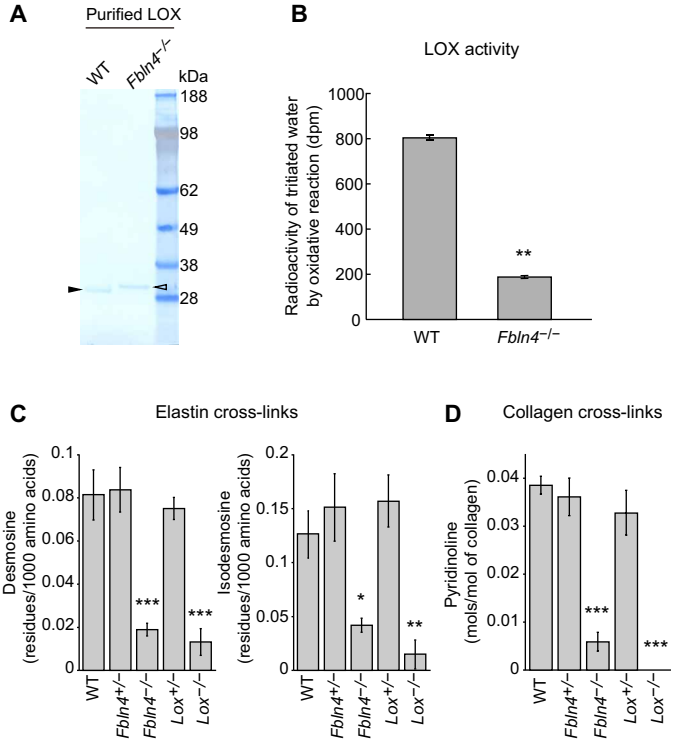

Fig. 3. Requirement of fibulin-4 for the enzymatic activity of LOX in vitro and in vivo. (**A**) Amido black staining of LOX protein purified from conditioned medium of WT and *Fbln4*$^{-/-}$ MEFs, transferred to a membrane after SDS-PAGE. Note that LOX from *Fbln4*$^{-/-}$ MEFs (open arrowhead) migrated slower by SDS-PAGE than that from WT MEFs (closed arrowhead). (**B**) Enzymatic activity of purified endogenous LOX from WT and *Fbln4*$^{-/-}$ MEFs. Bar graphs show mean ± SEM ($n = 4$). **$P < 0.01$. dpm, disintegration per minute. (**C** and **D**) Desmosine and isodesmosine (C) and pyridinoline (D) in neonatal aortae from each genotype. Four samples were collected for one analyte. Bar graphs show mean ± SEM ($n = 5$). *$P < 0.05$, **$P < 0.01$, and ***$P < 0.001$ compared with WT.

was not caused by an alternative propeptide cleavage site (fig. S1C). Similarly, the sulfation of LOX tyrosine residues does not account for the mobility shift, because YF mutant of LOX, in which potentially sulfated tyrosine residues were substituted by phenylalanine residues (*25*), showed a mobility shift similar to WT LOX when produced by *Fbln4*$^{-/-}$ MEFs (fig. S2).

To examine whether the LOX mobility shift was related to loss of LTQ formation, we mutated the lysine (K314A) or tyrosine (Y349A) residues that form LTQ. Figure 4A shows that either mutation introduced into LOX caused delayed migration by SDS-PAGE similar to that found with LOX produced by *Fbln4*$^{-/-}$ cells. Thus, the failure to form LTQ can cause the mobility shift. Quinoproteins are detected by staining with nitro blue tetrazolium (NBT), which is reduced to a colored formazan by the redox-cycling property of quinones (*26*). LOX purified from conditioned medium of WT MEFs, separated by SDS-PAGE and electroblotted to a membrane, was intensely stained by NBT. In contrast, staining of LOX produced by *Fbln4*$^{-/-}$ MEFs was largely diminished, suggesting that the latter contains much less LTQ (Fig. 4, B and C). Furthermore, LOX from *Fbln4*$^{-/-}$ MEFs appeared as two bands by amido black staining of the membrane, but only the minor lower band was stained by NBT (Fig. 4C). These data suggest that the lower band corresponds to LTQ-containing LOX, whereas the upper band is LOX that lacks LTQ. To directly measure LTQ levels, purified LOX was labeled with phenylhydrazine and digested with trypsin/Lys-C and Asp-N to generate the LTQ cross-link–containing peptide. Orbitrap mass spectrometric analysis (fig. S3) showed that the level of cross-linked peptide in the digest of LOX secreted from *Fbln4*$^{-/-}$ MEFs was markedly reduced compared to that in the digest of LOX secreted from WT MEFs (Fig. 4D). Together, these results indicate that fibulin-4 plays a necessary role in the formation of LTQ in LOX.

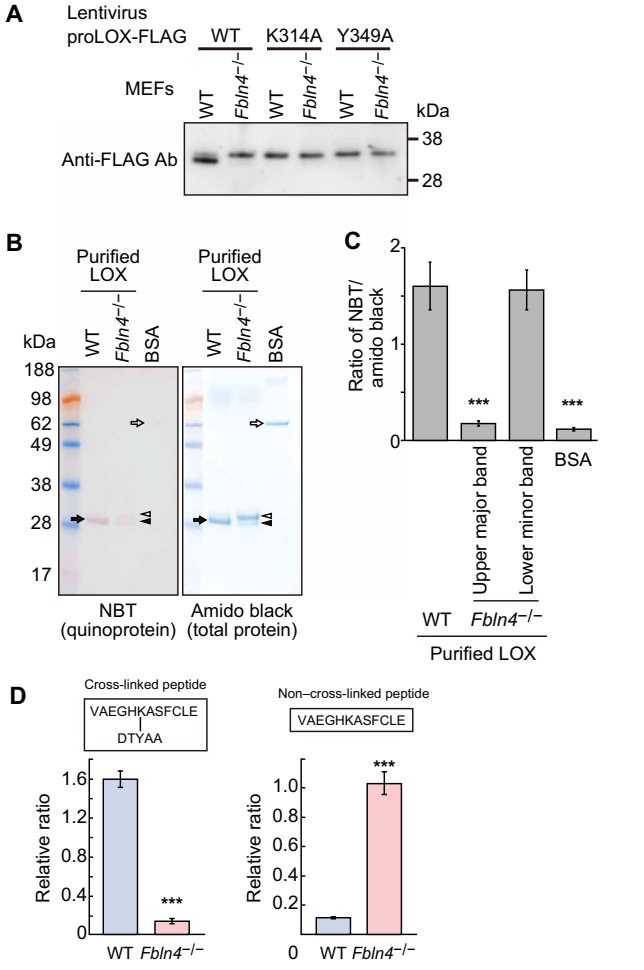

Fig. 4. Requirement of fibulin-4 for LTQ formation in LOX. (**A**) Western blot analysis of WT, K314A, and Y349A mutant LOX overexpressed and secreted from WT and *Fbln4*$^{-/-}$ MEFs. Note delayed migration of mutant LOX proteins even from WT MEFs. (**B** and **C**) Quinoprotein detection by NBT staining of membrane-transferred LOX (B, left) and total protein detection by amido black staining of the same membrane (B, right). BSA (open arrow) was used as a negative control for NBT staining. The major lower band of LOX from WT MEFs (closed arrow), the minor lower band of LOX from *Fbln4*$^{-/-}$ MEFs (closed arrowhead), and the major upper band of LOX from *Fbln4*$^{-/-}$ MEFs (open arrowhead) are indicated. The ratio of quantified density of each band was shown in (C). Bar graphs show mean ± SEM ($n = 4$). ***$P < 0.001$ compared with WT. (**D**) Relative quantification of cross-linked peptide derived from LTQ formation (left) and non–cross-linked peptide (right) by Orbitrap mass spectrometric analysis. The amounts of cross-linked peptide and non–cross-linked peptide were normalized to those of other LOX peptides. Bar graphs show mean ± SEM (triplicate measurements). ***$P < 0.001$.

Fibulin-4 promotes copper ion transfer from copper transporter ATP7A to proLOX

LTQ formation involves copper ion bound to specific histidine residues in proLOX (*5*). Copper loading occurs in the TGN and is dependent on the transfer of copper from the cytoplasm to proLOX in the lumen of the TGN by the copper transporter ATP7A (fig. S1A) (*5*, *6*). Therefore, we determined whether deficient LTQ formation in LOX produced by *Fbln4*$^{-/-}$ cells was due to reduced copper ion incorporation into proLOX. Endogenously expressed LOX from *Atp7a*$^{-/-}$ MEFs showed delayed migration in SDS-PAGE relative to LOX from WT MEFs, which was reversed by lentiviral expression of ATP7A (Fig. 5, A and B). Overexpressed LOX-FLAG from *Atp7a*$^{-/-}$ MEFs also showed delayed migration in SDS-PAGE similar to that from *Fbln4*$^{-/-}$ MEFs (Fig. 5C). In addition, LOX mutants in which copper-binding histidine residues were substituted by alanine residues to block copper binding showed similar mobility shift in SDS-PAGE, even when they were expressed by WT MEFs (Fig. 5D). Last, we measured copper ion bound to LOX purified from the culture medium of WT MEFs and *Fbln4*$^{-/-}$ MEFs, using inductively coupled plasma–mass spectrometry (ICP-MS). We found that copper ion bound to LOX produced by *Fbln4*$^{-/-}$ MEFs was markedly reduced compared to that produced by WT MEFs (Fig. 5E). These data suggest that loss of fibulin-4 causes a deficiency in copper ion incorporation into LOX, which results in defective LTQ formation.

To explore the mechanism by which fibulin-4 influences copper ion transfer from ATP7A to proLOX, we performed an in vitro binding assay using recombinant hemagglutinin (HA)–tagged fibulin-4 and FLAG-tagged ATP7A overexpressed by 293T cells. Our results showed interaction between the two proteins (Fig. 5F). Both the N-terminal and C-terminal FLAG-tagged halves of ATP7A interacted with HA-tagged fibulin-4 (fig. S4), suggesting that there are multiple binding sites for fibulin-4 within ATP7A. Protein mapping studies with fragments of fibulin-4 identified the middle cbEGF-like repeat (M domain) and the C-terminal fibulin-type motif (C domain) as the domains for binding to ATP7A. No interaction was found with the N-terminal domain of fibulin-4, indicating that the ATP7A-binding site resides in the M and C domain of fibulin-4 (Fig. 5G). These findings support a model where the N-terminal domain of fibulin-4 binds the propeptide domain of proLOX and the downstream M and C domains interact with ATP7A. In this way, fibulin-4 may function as a linker to facilitate direct copper ion transfer from ATP7A to proLOX (Fig. 6I).

Secreted fibulin-4 can be internalized by endocytosis and contribute to LTQ formation of LOX

An unexpected finding in our studies was the observation that low concentration (1 to 2 nM) of recombinant fibulin-4 added to culture medium reversed the mobility shift of LOX secreted by *Fbln4*$^{-/-}$ MEFs (Fig. 6A). The addition of 8 nM of recombinant fibulin-5, however, had no effect, nor did the N, M, or C fragment of fibulin-4 (fig. S5). Because ATP7A is not located on the cell surface in normal medium with low copper concentration (*27*), this result led us to hypothesize that exogenous fibulin-4 can be internalized and transported to the TGN lumen, where copper ion transfer to proLOX occurs (*27*). To test this hypothesis, we incubated MEF cells with recombinant FLAG-tagged fibulin-4 and anti-FLAG antibody at 4°C to inhibit internalization of the cell surface–bound protein. The cells were then warmed to 37°C to allow internalization of cell surface receptor–bound molecules. After acid washing to remove remaining cell surface proteins, internalized fibulin-4 was detected by immunofluorescent staining (Fig. 6, B to E). Internalization was partially inhibited by Dynasore, a dynamin inhibitor (*28*), and Filipin, an inhibitor of caveolae-mediated endocytosis (*29*), suggesting that fibulin-4 can be internalized by caveolae-mediated endocytosis. We cannot, however, exclude the possibility that fibulin-4 can also be internalized by clathrin-mediated endocytosis (Fig. 6F). To address whether exogenous fibulin-4 needs to be internalized to induce LTQ formation in LOX produced by *Fbln4*$^{-/-}$ MEFs, we added Dynasore in the same settings as Fig. 6A. The induction of LTQ formation by recombinant

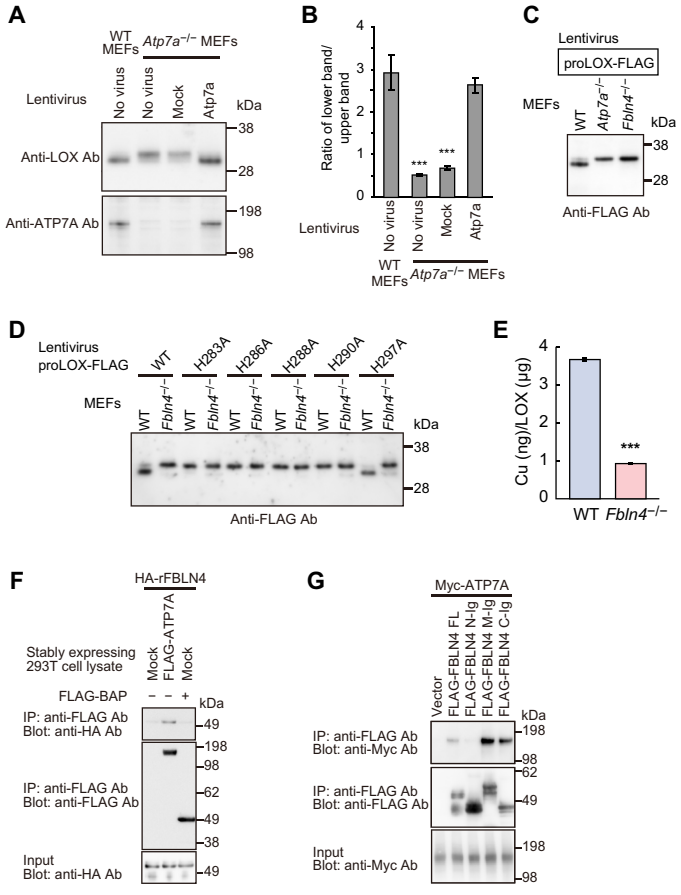

Fig. 5. Effect of deficient copper ion delivery on LOX mobility in SDS-PAGE and requirement of fibulin-4 for copper ion transfer from ATP7A to proLOX. (**A**) Western blot analysis of LOX endogenously expressed by WT and *Atp7a*$^{-/-}$ MEFs, with or without ATP7A overexpression by lentivirus. (**B**) Ratio of the quantified intensity of lower and upper bands of LOX. Bar graphs show mean ± SEM ($n = 3$). ***$P < 0.001$ compared with WT MEFs. (**C**) Western blot analysis of LOX-FLAG overexpressed by WT, *Atp7a*$^{-/-}$, and *Fbln4*$^{-/-}$ MEFs. (**D**) Western blot analysis of LOX-FLAG mutants, in which copper-binding histidines were substituted by alanines, secreted from WT and *Fbln4*$^{-/-}$ MEFs. (**E**) Quantification of copper incorporated in purified LOX by ICP-MS analysis. Bar graphs show mean ± SEM (triplicate measurements). ***$P < 0.001$. (**F**) An in vitro binding assay showing interaction of recombinant HA-tagged fibulin-4 and FLAG-tagged ATP7A overexpressed by 293T cells. FLAG-tagged bacterial alkaline phosphatase (FLAG-BAP) was used as a negative control. (**G**) In vitro binding assay for determining ATP7A-binding domain of fibulin-4. FLAG-tagged full-length fibulin-4 or the N, M, or C domain of fibulin-4 fused with immunoglobulin Fc region (Ig) was coimmunoprecipitated with Myc-tagged ATP7A.

fibulin-4 was significantly inhibited by Dynasore (Fig. 6G), and the levels of inhibition were comparable to that of endocytosis of fibulin-4 by the same concentration of Dynasore (Fig. 6F). Immunofluorescent staining of internalized fibulin-4 and the TGN marker Golgin-97 (*30*) revealed colocalization of these proteins (Fig. 6H). The cell surface attachment and the retrograde trafficking to the TGN were observed with full-length fibulin-4, but not with the N, M, or C fragment of fibulin-4 (fig. S6). These data suggest that some of the internalized fibulin-4 reaches the TGN, where copper ion transfer to proLOX occurs.

DISCUSSION

In the present study, we identified an essential role for fibulin-4 in the activation of LOX. Our proposed model is illustrated in Fig. 6I. Fibulin-4 interacts with ATP7A through its middle and C-terminal domain and thereby facilitates copper ion transfer from ATP7A to N-terminally bound proLOX. Because copper ion bound to specific histidine residues of proLOX is necessary for LTQ formation, fibulin-4 is crucial for generating active LOX. Without fibulin-4, the efficiency of copper ion transfer and subsequent LTQ formation are largely diminished (Fig. 5E), leading to production of inactive LOX.

We previously reported that the fibulin-4 interacts with LOX propeptide and with tropoelastin (*21*). This potential ability to bridge proLOX and tropoelastin could explain a part of the specific role for fibulin-4 in elastic fiber assembly; however, it cannot account for the nearly identical phenotypes of *Fbln4*$^{-/-}$ and *Lox*$^{-/-}$ mice that include collagen fiber abnormality in addition to elastic fiber deficiency (*10*, *11*, *19*). Our findings that fibulin-4 is necessary for LOX activity and that both elastin and collagen cross-links are greatly reduced in *Fbln4*$^{-/-}$ mouse tissues reconcile this phenotypic similarity.

Sasaki *et al.* (*20*) reported that osteoblasts from *Fbln4*$^{-/-}$ mice produce less mature LOX and suggested its mechanism as reduced processing of proLOX in the absence of fibulin-4. In our experiments with aortic tissues and MEFs with intact BMP-1, however, we did not observe the bands that correspond to unprocessed proLOX, in the absence or presence of fibulin-4 (fig. S7). Our data suggest that altered processing of proLOX is not a general mechanism by which the absence of fibulin-4 affects LOX activity.

In humans, homozygous or compound heterozygous mutations in the *FBLN4* gene are reported in autosomal recessive cutis laxa characterized by loose skin, arterial tortuosity and aneurysms, emphysema, and skeletal abnormality (*31*). Among these mutations, the E57K missense mutation is located at the N-terminal domain and is not assumed to affect the conformation of most of the protein (*32*). Homozygous *Fbln4* E57K mutant mice are reported to survive to adulthood and exhibit aortic aneurysm, arterial tortuosity, and emphysema, which recapitulate the human *FBLN4*$^{E57K/E57K}$ mutant phenotypes (*33*). Reduced binding of the E57K mutant fibulin-4 with proLOX (Fig. 1) and weak ability to induce LTQ formation in LOX (Fig. 2, B and C) are consistent with the less severe phenotypes of human and mouse mutants than those of *Fbln4*$^{-/-}$ mice.

Among the eight members of the fibulin family, fibulin-3, fibulin-4, and fibulin-5 share homology in sequence and domain configuration and are termed "short fibulins" or "elastogenic fibulins" because of their size and the phenotypes of the mice deficient in these genes (*31*). *Fbln5*$^{-/-}$ mice survive to adulthood and show stiff and tortuous arteries, emphysematous lungs, and loose skin, due to defective elastogenesis (*17*, *18*). Unlike *Fbln4* mutant mice, however, *Fbln5*$^{-/-}$ mice do not show aneurysms. We previously reported that fibulin-5 promotes coacervation of elastin and recruits elastin onto microfibrils (*34*). Considering that the loss of fibulin-5 is not compensated for by the presence of other fibulins including fibulin-4, these unique functions of fibulin-5 in elastic fiber assembly do not overlap with those of fibulin-4. Conversely, we reason that the role for fibulin-4 in the activation of LOX is not shared by other elastogenic fibulins, as fibulin-5 cannot interact with proLOX, and loss of fibulin-4 cannot be compensated for by the presence of other fibulins. However, it is possible that fibulin-5 also contributes to the formation of LTQ in LOXL1, because fibulin-5 interacts with LOXL1 and LOXL1 plays an important role in elastogenesis (*12*, *34*). The function of fibulin-3

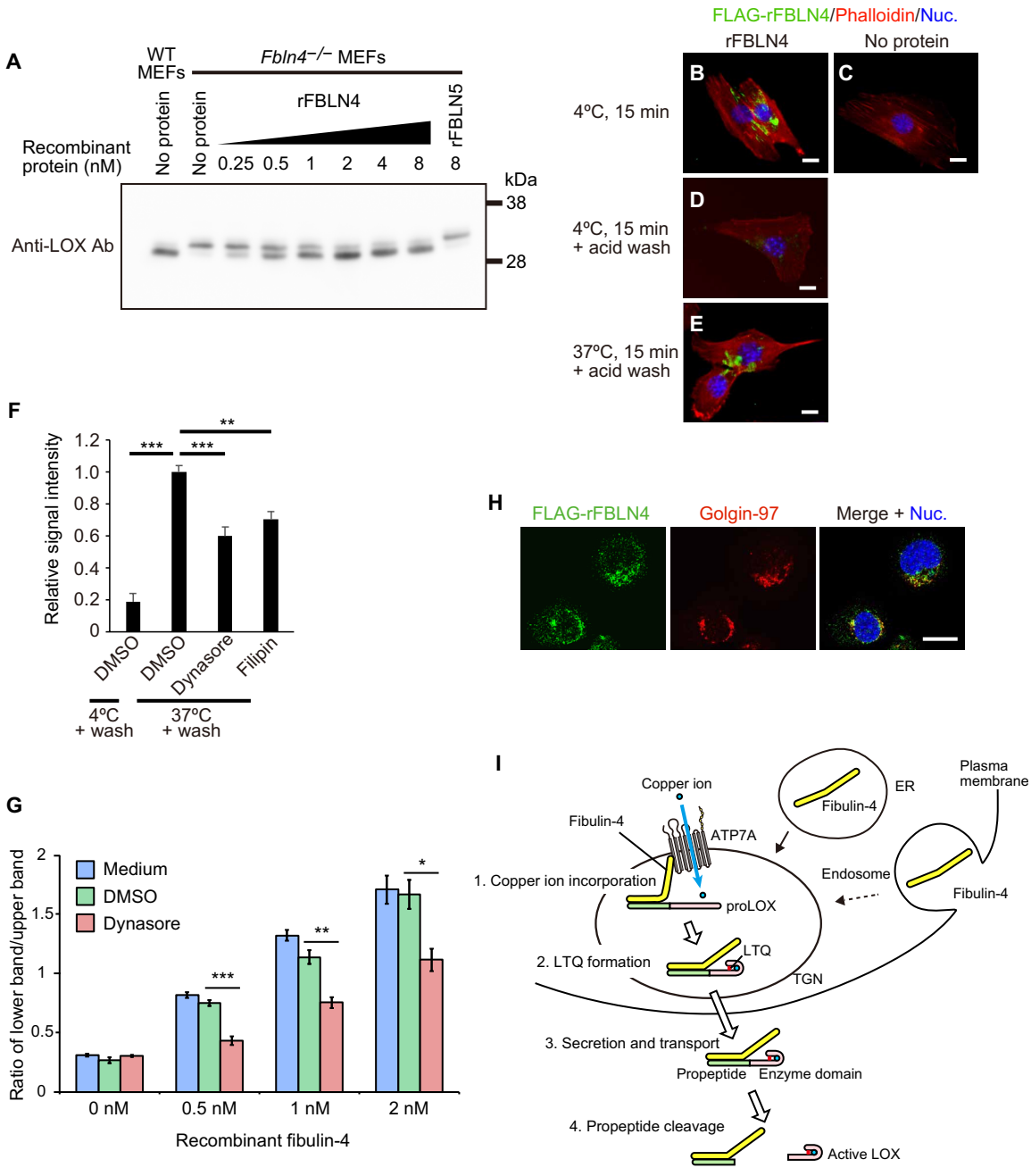

Fig. 6. Internalization of exogenous fibulin-4 and its function in LOX activation, and a model for the role of fibulin-4 in LOX activation. (**A**) Western blot analysis of LOX secreted from WT and *Fbln4*$^{-/-}$ MEFs, with or without addition of recombinant fibulin-4 (rFBLN4) in the medium. (**B** to **E**) Internalization of FLAG-rFBLN4 by *Fbln4*$^{-/-}$ MEFs. Cell surface–bound FLAG-rFBLN4 after 4°C incubation (B) could be removed by acid wash (D). The cells were warmed at 37°C followed by acid wash, and internalized FLAG-rFBLN4 was visualized (E). (**F**) Quantification of internalized FLAG-rFBLN4 with or without Dynasore (100 μM) and Filipin (2.5 μg/ml) treatment. Bar graphs show mean ± SEM ($n = 6$ to 8). $^{**}P < 0.01$ and $^{***}P < 0.001$ compared with dimethyl sulfoxide (DMSO). (**G**) Inhibition of rFBLN4-induced LTQ formation in LOX secreted from *Fbln4*$^{-/-}$ MEFs by Dynasore (100 μM). The ratio of the quantified intensity of lower and upper bands of LOX is shown. Bar graphs show mean ± SEM ($n = 3$). $^{*}P < 0.05$, $^{**}P < 0.01$, and $^{***}P < 0.001$ compared with DMSO. (**H**) Immunofluorescent staining showing colocalization of internalized FLAG-rFBLN4 and Golgin-97, a TGN marker. Scale bars, 10 μm. (**I**) A proposed model for the role of fibulin-4 in LOX activation. ER, endoplasmic reticulum.

is not clear, as *Fbln3*$^{-/-}$ mice show only minor elastic fiber defect in fascia (*35*).

Because the reduced LOX activity has been associated with mutations of the human or mouse *ATP7A* gene, copper incorporation into proLOX is assumed to be mediated by copper transporter ATP7A (*27*). However, a protein that functions to mediate the transfer of copper from ATP7A to proLOX has not been anticipated. We showed that fibulin-4 promotes copper ion transfer from ATP7A to proLOX in the Golgi, which is a necessary step for generation of LTQ, a critical cofactor for the oxidase activity. Our studies suggest the existence of similar bridging proteins for other copper-dependent enzymes, too, such as tyrosinase or peptidylglycine α-amidating

monooxygenase, enzymes necessary for melanin production or prohormone maturation, respectively (*27*). How fibulin-4 affects copper transfer is not yet known. We cannot exclude the possibility that binding with fibulin-4 alters the conformation of proLOX so that it can incorporate copper ion, which does not necessarily contradict with the bridging model shown in Fig. 6I. Further study is needed to examine this possibility.

The finding that the addition of recombinant fibulin-4 to cell culture medium could promote the formation of LTQ in LOX was unexpected, because copper transfer to proLOX and subsequent LTQ formation occurs in the TGN (*27*). Very low concentrations (1 to 2 nM) of fibulin-4 in the medium were sufficient to induce LTQ formation in LOX, suggesting that fibulin-4 may work as a circulating factor for LOX activation. There is a report showing that high serum levels of fibulin-4 are associated with ovarian cancer (normal ~30 ng/ml versus cancer ~300 ng/ml) (*36*). This reported normal level of fibulin-4 (~30 ng/ml = ~0.6 nM) corresponds to a concentration that can partially (~50%) induce LTQ formation in LOX (Fig. 6A). Identification of the receptor for fibulin-4 for endocytosis and measuring the concentrations of fibulin-4 in circulating blood in various ages and in developmental stages require further investigation. It would also be interesting to see whether ectopic expression of fibulin-4 could rescue the phenotypes of *Fbln4*$^{-/-}$ mice to understand the role for circulating fibulin-4 in vivo.

Together, our results show that fibulin-4 is essential for the formation of enzymatically active LOX and, hence, for elastic fiber formation and collagen fibrillogenesis. Endogenously expressed fibulin-4 or endocytosed fibulin-4 that is transported to the TGN promotes copper ion transfer from ATP7A to proLOX, which is necessary for the formation of LTQ, an intramolecular cross-link that works as a cofactor for the oxidase activity of LOX (Fig. 6I). Our findings provide insights into the mechanism of ECM maturation and diseases that involve fibrosis or insufficient elastogenesis.

MATERIALS AND METHODS

Mice

All mice used here were maintained on normal laboratory diet. *Fbln4*$^{-/-}$, *Fbln5*$^{-/-}$, and *Lox*$^{-/-}$ mice were previously described (*19*, *17*, *10*) and maintained in Kansai Medical University. All procedures were approved by the Committee for Animal Experiments of Kansai Medical University and conducted according to the Guideline for Animal Experimentation at Kansai Medical University.

Antibodies

Primary antibodies used were anti-FLAG (Sigma-Aldrich, F1804), anti-Myc and anti-HA (Medical & Biological Laboratories Co., M192-3S and M180-3, respectively), anti-LOX (Abcam, ab31238), anti-ATP7A (Abcam, ab13995), and anti–Golgin-97 (Cell Signaling Technology, 13192) antibodies. Secondary antibodies used were horseradish peroxidase–conjugated anti-mouse immunoglobulin G (IgG), anti-rabbit IgG, and anti-chicken IgY (Abcam, ab205719, ab6721, and ab6877, respectively) and Alexa Fluor 488–conjugated anti-mouse IgG and Alexa Fluor 555–conjugated anti-rabbit IgG (Thermo Fisher Scientific, A-11029 and A-31572, respectively).

Cell culture and genome editing

MEFs and 293T cells were maintained in Advanced DMEM (Dulbecco's modified Eagle's medium) (Thermo Fisher Scientific) supplemented with 2 mM glutamine, penicillin/streptomycin (100 U/100 mg ml^{-1}), and 5% fetal bovine serum at 37°C in 5% CO_2. MEFs were harvested from WT and *Fbln4*$^{-/-}$ mouse embryo and immortalized by transferring with human telomere reverse transcriptase cDNA. For the purification of endogenous LOX from MEFs, a monoclonal cell line expressing high-level LOX was selected by limiting dilution of immortalized WT MEFs, followed by *Fbln4* gene deletion using the CRISPR-Cas9 system with double-nicking strategy (*37*). *Fbln4* single-guide RNA (sgRNA) pairs (5′-agagcagcaaagacccgggg-3′ and 5′-ggcgtttctgctgttgctct-3′) were cloned into Bbs I–digested plasmid pX335 (42335, Addgene). The plasmids were transduced into WT MEFs followed by clonal isolation and expansion. Targeted region was amplified from genomic DNA, and indel mutations were validated by Sanger sequencing. *Atp7a*$^{-/-}$ MEFs were generated in the same manner using *Atp7a* sgRNA pairs (5′-aacagtcaggaacacggtat-3′ and 5′-ctgctccactgactctgcct-3′). To obtain *BMP1*$^{-/-}$ 293T cells and *Bmp1*$^{-/-}$ MEFs, *BMP1* sgRNA pairs (5′-cgacgacgtggcccagctcg-3′ and 5′-cgaacacactcggccagacc-3′) and *Bmp1* sgRNA pairs (5′-gggccacacccgctccggtc-3′ and 5′-ggggtcatcccgtttgtgat-3′) were used, respectively.

Plasmid construction, lentiviral gene transfer, and protein purification

FBLN4-WT, *FBLN5*, and *LOX* cDNA were subcloned as previously described (*21*, *34*). *FBLN4-E57K*, *FBLN4-ΔN1* (ΔQ28-R53), *FBLN4-ΔN2* (ΔD54-V122), *FBLN4-N* (Q28-V122), *FBLN4-M* (D123-R314), *FBLN4-C* (C315-F443), *Lox-WT*, *Lox-K314A*, *Lox-Y349A*, *Lox-H283A*, *Lox-H286A*, *Lox-H288A*, *Lox-H290A*, *Lox-H297A*, *Fbln4-FL*, *Fbln4-N* (Q47-V141), *Fbln4-M* (D142-R333), *Fbln4-C* (C334-F462), and *ATP7A* cDNA were amplified by polymerase chain reaction (PCR) and subcloned into pENTR/ssHA, pENTR/ssbFLAG, pENTR/cFLAG, pEF6/ssFLAG, pEF6/ssFLAG-hIgG, pENTR/atgFLAG, and pENTR/atgMyc. *Atp7a* cDNA was synthesized (Thermo Fisher Scientific) to generate silent mutations to stabilize this gene in high-copy plasmid during replication in *Escherichia coli* (*38*) and subcloned into pENTR/atgFLAG. *Atp7a-TM1–4* (ΔK794-L1397) and *Atp7a-TM5–8* (ΔF646-D927) cDNA were amplified by PCR and subcloned into pENTR/atgFLAG. YF mutant *Lox* cDNA, in which all potentially sulfated tyrosine residues (Y177, Y178, Y180, Y181, and Y184) of mouse LOX were substituted by phenylalanine residues (*25*), was generated by PCR-based mutagenesis using pENTR-*Lox*-cFLAG as a template. The entry clones were recombined with pLenti6.3 destination vectors using Gateway Technology (Invitrogen). Lentiviral particles were produced via cotransfection of 293T cells with the packaging plasmids using PEI MAX (Polysciences). Supernatants were collected starting from 40 hours after transfection for 24 to 48 hours and concentrated using Lenti-X Concentrator (Clontech) according to the manufacturer's instructions. The resulting viral pellet was resuspended in culture medium at ~$^1/_{10}$ of the original volume, and the viral aliquot was stored frozen. Using Ni-NTA affinity resin (Qiagen), recombinant fibulin-4 or fibulin-5 was purified from serum-free conditioned medium of 293T cells stably expressing fibulin-4 or fibulin-5 with N-terminal His-tags (*21*, *34*).

In vitro binding assay

293T cells were transfected with the plasmids using PEI MAX (Polysciences). The transfected cells were cultured in serum-free DMEM/F12 (Thermo Fisher Scientific). The conditioned medium (proLOX) or the cell lysates (ATP7A) and fibulin-4 and its mutants (recombinant

protein or conditioned medium) were mixed and subjected to immunoprecipitation with anti-FLAG M2 affinity gel (Sigma-Aldrich) followed by SDS-PAGE with NuPAGE Bis-Tris acrylamide gel (4 to 12%) and MOPS or MES buffer (Thermo Fisher Scientific) and Western blotting as described previously (*39*). N-terminal FLAG-tagged bacterial alkaline phosphatase (FLAG-BAP) fusion protein was purchased from Sigma-Aldrich.

Immunodetection of endogenous and FLAG-tagged LOX

Proteins were extracted from mouse neonatal aorta tissues with 8 M urea solution, and supernatants were collected. Equal loadings of protein extracts were subjected to SDS-PAGE with NuPAGE Bis-Tris acrylamide gel (4 to 12%) and MES buffer (Thermo Fisher Scientific), followed by Western blotting. Cultured MEFs were infected by lentiviral particles with the volume adjusted individually to secrete equivalent amount of recombinant proteins. The supernatants of MEFs were replaced by serum-free Advanced DMEM/F12 (Thermo Fisher Scientific) on the next day of infection and harvested at 48 to 72 hours after replacement. The endogenous and FLAG-tagged LOX in the medium were concentrated using DEAE Sepharose Fast Flow (GE Healthcare), followed by SDS-PAGE with NuPAGE Bis-Tris acrylamide gel (4 to 12%) and MES buffer (Thermo Fisher Scientific) and Western blotting. For quantification, blots were scanned, and the integral density of specific bands was measured using Image Gauge Ver. 4.22.

Purification of endogenous LOX and N-terminal amino acid sequence

For the purification of endogenous mature LOX from the culture medium, DEAE Sepharose Fast Flow was added to the medium. After several hours of incubation followed by washing, the DEAE-bound LOX was eluted by 1 M NaCl and 6 M urea in 10 mM phosphate buffer (PB). The eluates were dialyzed with PB, followed by separation using Sephacryl S-200 HR (GE Healthcare) that works as an affinity column for LOX (*40*). After washing, LOX was eluted with 6 M urea in PB. The eluates were concentrated by ultrafiltration. The concentration of purified LOX was quantified as described previously (*39*).

Purified LOX protein was electrophoresed on a 4 to 12% SDS–polyacrylamide gel and then transferred onto a polyvinylidene difluoride (PVDF) membrane operated at 30 V for 1 hour. After the membrane was stained with SimplyBlue SafeStain (Thermo Fisher Scientific), the purified LOX band was excised and analyzed using a PPSQ-33A amino acid sequencer system (Shimadzu).

Enzymatic activity measurement of LOX

Rates of oxidation of peptidyl lysine were assessed using the tritiated recombinant human tropoelastin as substrates, as described previously (*41*) with some modifications. Plasmids encoding human tropoelastin cDNA (pTrc His3-hELN) were transformed into One Shot Stbl3 Chemically Competent *E. coli* (Thermo Fisher Scientific). A 10-ml aliquot of an overnight culture of bacteria was diluted in 90 ml of LB medium containing ampicillin (50 μg ml^{-1}), and the freshly inoculated culture was incubated with shaking at 37°C overnight. The cells were collected and washed twice with phosphate-buffered saline (PBS) by centrifugation; the cell pellet was suspended in 160 ml of lysine-free RPMI 1640 medium (Sigma-Aldrich) with 1.15 mM arginine, 0.38 mM leucine, [L-4,5-^{3}H]lysine (1.6 mCi/liter; 80 to 110 Ci $mmol^{-1}$), and 2 mM isopropyl-β-D(−)-thiogalactopyranoside (Wako Pure Chemical) and incubated in this medium with shaking at 37°C for 8 hours. The labeled cells were isolated by centrifugation and dissolved in 8 M urea/PBS (pH 7.4) with stirring overnight at 4°C. The suspension was centrifuged (10,000*g*, 30 min, 4°C), and the supernatant was loaded onto a HisTrap FF (GE Healthcare Life Sciences) equilibrated with binding buffer [8 M urea/PBS (pH 7.4)] at 5.0 ml/min. The bound protein was eluted with elution buffer (binding buffer containing 200 mM imidazole). The eluate was dialyzed overnight against PBS with Slide-A-Lyzer Dialysis Cassette 10K MWCO (Thermo Fisher Scientific), concentrated to 20,000 cpm/μl using Amicon Ultra 30K centrifugal filter devices (Merck Millipore), and used for lysine oxidation assay.

Assay mixtures included purified LOX protein and 200,000 cpm of the elastin substrate suspended or dissolved in 0.1 M sodium borate and 0.15 M NaCl (pH 8.0) in a total volume of 0.8 ml and were incubated for 2 hours at 37°C. Tritiated water formed during the incubation was isolated from the elastin substrate by the trichloroacetic acid precipitation method, and radioactivity in 0.7-ml aliquot of the supernatants was quantified by liquid scintillation spectrometry. The radioactivity was corrected for each enzyme-free control, and all enzyme activities in the assay mixtures were ≥90% inhibited by the inclusion of 50 μM β-aminopropionitrile, a specific inhibitor of LOX.

Collagen and elastin cross-link analysis

The dissected aortae (n = 5 per genotype; four samples were pooled for a single analysis) were subjected to amino acid analysis and elastin and collagen cross-link analyses as described (*42*). Briefly, the samples were pulverized in liquid nitrogen, washed with cold PBS and cold distilled water by repeated centrifugation at 4000*g* for 30 min, and lyophilized. An aliquot of each (~2 mg) was hydrolyzed with 6 N HCl and subjected to amino acid analysis. Desmosine and isodesmosine were quantified as residues per 1000 amino acids based on the commercially available standards. Aliquots of the hydrolysates with known amounts of hydroxyproline were also subjected to collagen cross-link analysis. The major nonreducible cross-link pyridinoline was quantified as moles/mole of collagen.

NBT and amido black staining of the membrane

For NBT staining, the PVDF membrane with transferred protein was immersed in 0.24 mM NBT (Wako Pure Chemical) in 2 M potassium glycinate solution (pH 10.0) for 45 min in the dark. For amido black staining, the membrane was stained with 0.1% amido black (Wako Pure Chemical) in 45% methanol/10% acetic acid for 1 min, followed by destaining with 90% methanol/2% acetic acid three times for 1 min each. The intensity of stained bands was quantified using ImageJ software [National Institutes of Health (NIH), Bethesda, MD].

Detection and quantification of cross-linked and non–cross-linked fragment of LOX

Purified LOX was incubated with 1 mM phenylhydrazine at 25°C for 1 hour and 37°C for 30 min, followed by dialysis with 2 M urea in PB. After adding ammonium bicarbonate to a concentration of 50 mM to 0.2 μg of LOX solution, disulfide bonds were reduced by adding dithiothreitol to a concentration of 50 mM and incubating at 56°C for 1 hour. Subsequently, free sulfhydryl groups were alkylated by adding iodoacetamide to a concentration of 50 mM and incubating at 25°C for 1 hour. After these modifications, protein

digestion with Asp-N (Takara Bio) and Trypsin/Lys-C Protease Mix (Thermo Fisher Scientific) was performed. To stop digestion, trifluoroacetic acid was added to a concentration of 1%.

The ultra-high performance liquid chromatography–MS/MS analysis was performed on Q Exactive HF-X Hybrid Quadrupole-Orbitrap Mass Spectrometer (Thermo Fisher Scientific) equipped with Easy-nLC 1200 (Thermo Fisher Scientific). Chromatographic separation of targeted analytes was achieved on PepMap100 C18 LC Column (75-μm inner diameter, 3-μm particle, 100-Å pore size; Thermo Fisher Scientific). Solvent A contained 0.1% formic acid, and solvent B contained 80% acetonitrile and 0.1% formic acid. Peptides were separated through a solvent B gradient from 4 to 100% within 75 min at a flow rate of 0.3 μl/min. Using MS/MS analysis, we determined that two peaks of mass/charge ratio (*m/z*) 994.9440 (+2) and 663.6318 (+3) were derived from cross-linked peptide VAEGHKASFCLE-DTYAA with modification of phenylhydrazine labeling and carbamidomethylation on cysteine, and a peak of *m/z* 695.8256 (+2) was derived from non–cross-linked peptide VAEGHKASFCLE with modification of carbamidomethylation on cysteine and carbamylation on lysine. To evaluate the total amount of LOX for normalization, we selected seven peptides: DYGYHR (+2), *m/z* 405.67987; DYTNNVVR (+2), *m/z* 490.74481; DFLPSRPR (+2), *m/z* 494.2746; DEFSHY (+2), *m/z* 399.15863; DVQPGNYILK (+2), *m/z* 573.81238; DPYYIQASTYVQK (+2), *m/z* 788.38885; and NRPGYGTGYFQYGLP (+2), *m/z* 845.40326. Relative intensity of each peak was quantified by targeted single ion monitoring using extracted ion chromatography. Peak area of each ion was measured in triplicate. Relative intensities of cross-linked and non–cross-linked peptides were normalized to the average intensities of the seven LOX peptides.

Determination of Cu concentration by ICP-MS

A 30-μl aliquot of samples was wet-ashed with 50 μl of nitric acid (analytical grade, Wako Pure Chemical Industries) on a hot plate. The samples were then diluted with 1% nitric acid to 300 μl, followed by measurement using an inductively coupled plasma mass spectrometer (ICP-MS; Agilent 8800, Agilent Technologies). The signal intensities of Cu were monitored at *m/z* 65 with the integration time of 0.1 s, and the Cu concentration was calculated using a standard calibration method.

Immunocytochemistry

Fbln4$^{-/-}$ MEFs were seeded on a glass-bottom dish. The next day, the cells were incubated with culture medium containing recombinant FLAG-FBLN4 (40 nM) with or without endocytosis inhibitors Dynasore (Santa Cruz Biotechnology) and Filipin (LKT Laboratories). The inhibitors were present in all steps except for the washing buffer. After 3 hours of incubation, the cells were placed on ice and washed with ice-cold PBS. After 5 min, the cell surface–bound FLAG-FBLN4 was labeled by incubating the cells with ice-cold culture medium containing anti-FLAG antibody. After incubation for 30 min on ice, the cells were washed twice with ice-cold PBS and then incubated with warm culture medium at 37°C to allow the internalization. The internalization was stopped by placing the cells on ice and washing with ice-cold PBS. To remove uninternalized cell surface–bound antibodies, the cells were washed with ice-cold acid wash buffer containing 50 mM glycine and 150 mM NaCl (pH 2.0) for 1 min, followed by washing with PBS to neutralize the pH. The cells were then fixed with 4% paraformaldehyde, washed with PBS, permeabilized with 1% Triton X-100, and blocked with 5% bovine serum albumin (BSA)/PBS for 1 hour. To visualize cell surface and internalized anti-FLAG antibody bound to FLAG-FBLN4, a fluorescence-conjugated secondary antibody was used. The cells were observed using a BZ-9000 microscope (Keyence) and an LSM 700 microscope (Zeiss). Intensity of the signal was quantified using ArrayScan VTI (Thermo Fisher Scientific).

Statistics

Comparisons were made using Student's *t* test between two groups. Analyses across multiple groups were made using a one-way analysis of variance (ANOVA) with Dunnett's multiple comparisons post hoc test. *P* values less than 0.05 were considered to be significant.

SUPPLEMENTARY MATERIALS

Supplementary material for this article is available at http://advances.sciencemag.org/cgi/content/full/6/48/eabc1404/DC1

View/request a protocol for this paper from *Bio-protocol*.

REFERENCES AND NOTES

1. J. Rosenbloom, W. R. Abrams, R. Mecham, Extracellular matrix 4: The elastic fiber. *FASEB J.* **7**, 1208–1218 (1993).
2. M. Yamauchi, M. Sricholpech, Lysine post-translational modifications of collagen. *Essays Biochem.* **52**, 113–133 (2012).
3. D. R. Eyre, M. A. Paz, P. M. Gallop, Cross-linking in collagen and elastin. *Annu. Rev. Biochem.* **53**, 717–748 (1984).
4. K. Reiser, R. J. McCormick, R. B. Rucker, Enzymatic and nonenzymatic cross-linking of collagen and elastin. *FASEB J.* **6**, 2439–2449 (1992).
5. S. X. Wang, M. Mure, K. F. Medzihradszky, A. L. Burlingame, D. E. Brown, D. M. Dooley, A. J. Smith, H. M. Kagan, J. P. Klinman, A crosslinked cofactor in lysyl oxidase: Redox function for amino acid side chains. *Science* **273**, 1078–1084 (1996).
6. R. B. Rucker, T. Kosonen, M. S. Clegg, A. E. Mitchell, B. R. Rucker, J. Y. Uriu-Hare, C. L. Keen, Copper, lysyl oxidase, and extracellular matrix protein cross-linking. *Am. J. Clin. Nutr.* **67**, 996S–1002S (1998).
7. M. I. Uzel, I. C. Scott, H. Babakhanlou-Chase, A. H. Palamakumbura, W. N. Pappano, H.-H. Hong, D. S. Greenspan, P. C. Trackman, Multiple bone morphogenetic protein 1-related mammalian metalloproteinases process pro-lysyl oxidase at the correct physiological site and control lysyl oxidase activation in mouse embryo fibroblast cultures. *J. Biol. Chem.* **276**, 22537–22543 (2001).
8. H. A. Lucero, H. M. Kagan, Lysyl oxidase: An oxidative enzyme and effector of cell function. *Cell. Mol. Life Sci.* **63**, 2304–2316 (2006).
9. Y. Zhao, C. Min, S. R. Vora, P. C. Trackman, G. E. Sonenshein, K. H. Kirsch, The lysyl oxidase pro-peptide attenuates fibronectin-mediated activation of focal adhesion kinase and p130^{Cas} in breast cancer cells. *J. Biol. Chem.* **284**, 1385–1393 (2009).
10. I. K. Hornstra, S. Birge, B. Starcher, A. J. Bailey, R. P. Mecham, S. D. Shapiro, Lysyl oxidase is required for vascular and diaphragmatic development in mice. *J. Biol. Chem.* **278**, 14387–14393 (2003).
11. J. M. Mäki, J. Räsänen, H. Tikkanen, R. Sormunen, K. Mäkikallio, K. I. Kivirikko, R. Soininen, Inactivation of the lysyl oxidase gene *Lox* leads to aortic aneurysms, cardiovascular dysfunction, and perinatal death in mice. *Circulation* **106**, 2503–2509 (2002).
12. X. Liu, Y. Zhao, J. Gao, B. Pawlyk, B. Starcher, J. A. Spencer, H. Yanagisawa, J. Zuo, T. Li, Elastic fiber homeostasis requires lysyl oxidase-like 1 protein. *Nat. Genet.* **36**, 178–182 (2004).
13. A. Martin, F. Salvador, G. Moreno-Bueno, A. Floristán, C. Ruiz-Herguido, E. P. Cuevas, S. Morales, V. Santos, K. Csiszar, P. Dubus, J. J. Haigh, A. Bigas, F. Portillo, A. Cano, Lysyl oxidase-like 2 represses Notch1 expression in the skin to promote squamous cell carcinoma progression. *EMBO J.* **34**, 1090–1109 (2015).
14. J. Zhang, R. Yang, Z. Liu, C. Hou, W. Zong, A. Zhang, X. Sun, J. Gao, Loss of lysyl oxidase-like 3 causes cleft palate and spinal deformity in mice. *Hum. Mol. Genet.* **24**, 6174–6185 (2015).
15. H. M. Kagan, W. Li, Lysyl oxidase: Properties, specificity, and biological roles inside and outside of the cell. *J. Cell. Biochem.* **88**, 660–672 (2003).
16. P. Bornstein, Matricellular proteins: An overview. *J. Cell Commun. Signal.* **3**, 163–165 (2009).
17. T. Nakamura, P. R. Lozano, Y. Ikeda, Y. Iwanaga, A. Hinek, S. Minamisawa, C.-F. Cheng, K. Kobuke, N. Dalton, Y. Takada, K. Tashiro, J. Ross Jr., T. Honjo, K. R. Chien, Fibulin-5/DANCE is essential for elastogenesis in vivo. *Nature* **415**, 171–175 (2002).

18. H. Yanagisawa, E. C. Davis, B. C. Starcher, T. Ouchi, M. Yanagisawa, J. A. Richardson, E. N. Olson, Fibulin-5 is an elastin-binding protein essential for elastic fibre development in vivo. *Nature* **415**, 168–171 (2002).
19. P. J. McLaughlin, Q. Chen, M. Horiguchi, B. C. Starcher, J. B. Stanton, T. J. Broekelmann, A. D. Marmorstein, B. McKay, R. Mecham, T. Nakamura, L. Y. Marmorstein, Targeted disruption of fibulin-4 abolishes elastogenesis and causes perinatal lethality in mice. *Mol. Cell. Biol.* **26**, 1700–1709 (2006).
20. T. Sasaki, R. Stoop, T. Sakai, A. Hess, R. Deutzmann, U. Schlötzer-Schrehardt, M.-L. Chu, K. von der Mark, Loss of fibulin-4 results in abnormal collagen fibril assembly in bone, caused by impaired lysyl oxidase processing and collagen cross-linking. *Matrix Biol.* **50**, 53–66 (2016).
21. M. Horiguchi, T. Inoue, T. Ohbayashi, M. Hirai, K. Noda, L. Y. Marmorstein, D. Yabe, K. Takagi, T. O. Akama, T. Kita, T. Kimura, T. Nakamura, Fibulin-4 conducts proper elastogenesis via interaction with cross-linking enzyme lysyl oxidase. *Proc. Natl. Acad. Sci. U.S.A.* **106**, 19029–19034 (2009).
22. V. Hucthagowder, N. Sausgruber, K. H. Kim, B. Angle, L. Y. Marmorstein, Z. Urban, Fibulin-4: A novel gene for an autosomal recessive cutis laxa syndrome. *Am. J. Hum. Genet.* **78**, 1075–1080 (2006).
23. P. C. Trackman, D. Bedell-Hogan, J. Tang, H. M. Kagan, Post-translational glycosylation and proteolytic processing of a lysyl oxidase precursor. *J. Biol. Chem.* **267**, 8666–8671 (1992).
24. A. D. Cronshaw, L. A. Fothergill-Gilmore, D. J. S. Hulmes, The proteolytic processing site of the precursor of lysyl oxidase. *Biochem. J.* **306**, 279–284 (1995).
25. T. Rosell-García, A. Paradela, G. Bravo, L. Dupont, M. Bekhouche, A. Colige, F. Rodriguez-Pascual, Differential cleavage of lysyl oxidase by the metalloproteinases BMP1 and ADAMTS2/14 regulates collagen binding through a tyrosine sulfate domain. *J. Biol. Chem.* **294**, 11087–11100 (2019).
26. M. A. Paz, R. Flückiger, A. Boak, H. M. Kagan, P. M. Gallop, Specific detection of quinoproteins by redox-cycling staining. *J. Biol. Chem.* **266**, 689–692 (1991).
27. S. Lutsenko, A. Gupta, J. L. Burkhead, V. Zuzel, Cellular multitasking: The dual role of human Cu-ATPases in cofactor delivery and intracellular copper balance. *Arch. Biochem. Biophys.* **476**, 22–32 (2008).
28. E. Macia, M. Ehrlich, R. Massol, E. Boucrot, C. Brunner, T. Kirchhausen, Dynasore, a cell-permeable inhibitor of dynamin. *Dev. Cell* **10**, 839–850 (2006).
29. K. G. Rothberg, Y. S. Ying, B. A. Kamen, R. G. Anderson, Cholesterol controls the clustering of the glycophospholipid-anchored membrane receptor for 5-methyltetrahydrofolate. *J. Cell Biol.* **111**, 2931–2938 (1990).
30. L. Kjer-Nielsen, R. D. Teasdale, C. van Vliet, P. A. Gleeson, A novel Golgi-localisation domain shared by a class of coiled-coil peripheral membrane proteins. *Curr. Biol.* **9**, 385–390 (1999).
31. T. Nakamura, Roles of short fibulins, a family of matricellular proteins, in lung matrix assembly and disease. *Matrix Biol.* **73**, 21–33 (2018).
32. T. Sasaki, F.-G. Hanisch, R. Deutzmann, L. Y. Sakai, T. Sakuma, T. Miyamoto, T. Yamamoto, E. Hannappel, M.-L. Chu, H. Lanig, K. von der Mark, Functional consequence of fibulin-4 missense mutations associated with vascular and skeletal abnormalities and cutis laxa. *Matrix Biol.* **56**, 132–149 (2016).
33. O. Igoucheva, V. Alexeev, C. M. Halabi, S. M. Adams, I. Stoilov, T. Sasaki, M. Arita, A. Donahue, R. P. Mecham, D. E. Birk, M.-L. Chu, Fibulin-4 E57K knock-in mice recapitulate cutaneous, vascular and skeletal defects of recessive cutis laxa 1B with both elastic fiber and collagen fibril abnormalities. *J. Biol. Chem.* **290**, 21443–21459 (2015).
34. M. Hirai, T. Ohbayashi, M. Horiguchi, K. Okawa, A. Hagiwara, K. R. Chien, T. Kita, T. Nakamura, Fibulin-5/DANCE has an elastogenic organizer activity that is abrogated by proteolytic cleavage in vivo. *J. Cell Biol.* **176**, 1061–1071 (2007).
35. P. J. McLaughlin, B. Bakall, J. Choi, Z. Liu, T. Sasaki, E. C. Davis, A. D. Marmorstein, L. Y. Marmorstein, Lack of fibulin-3 causes early aging and herniation, but not macular degeneration in mice. *Hum. Mol. Genet.* **16**, 3059–3070 (2007).
36. J. Chen, Z. Liu, S. Fang, R. Fang, X. Liu, Y. Zhao, X. Li, L. Huang, J. Zhang, Fibulin-4 is associated with tumor progression and a poor prognosis in ovarian carcinomas. *BMC Cancer* **15**, 91 (2015).
37. F. A. Ran, P. D. Hsu, J. Wright, V. Agarwala, D. A. Scott, F. Zhang, Genome engineering using the CRISPR-Cas9 system. *Nat. Protoc.* **8**, 2281–2308 (2013).
38. S. Zhu, V. Shanbhag, V. L. Hodgkinson, M. J. Petris, Multiple di-leucines in the ATP7A copper transporter are required for retrograde trafficking to the trans-Golgi network. *Metallomics* **8**, 993–1001 (2016).
39. K. Noda, B. Dabovic, K. Takagi, T. Inoue, M. Horiguchi, M. Hirai, Y. Fujikawa, T. O. Akama, K. Kusumoto, L. Zilberberg, L. Y. Sakai, K. Koli, M. Naitoh, H. von Melchner, S. Suzuki, D. B. Rifkin, T. Nakamura, Latent TGF-β binding protein 4 promotes elastic fiber assembly by interacting with fibulin-5. *Proc. Natl. Acad. Sci. U.S.A.* **110**, 2852–2857 (2013).
40. D. R. Shackleton, D. J. Hulmes, Purification of lysyl oxidase from piglet skin by selective interaction with Sephacryl S-200. *Biochem. J.* **266**, 917–919 (1990).
41. D. Bedell-Hogan, P. Trackman, W. Abrams, J. Rosenbloom, H. Kagan, Oxidation, cross-linking, and insolubilization of recombinant tropoelastin by purified lysyl oxidase. *J. Biol. Chem.* **268**, 10345–10350 (1993).
42. M. Yamauchi, Y. Taga, S. Hattori, M. Shiiba, M. Terajima, Analysis of collagen and elastin cross-links. *Methods Cell Biol.* **143**, 115–132 (2018).

Acknowledgments: We thank M. Masuda and C. Murabe for technical assistance and Y. Nagashima (Thermo Fisher Scientific) for MS analysis. **Funding:** This work was supported by the Funding Program for Next Generation World-Leading Researchers in Japan (LS120), Japan Society for the Promotion of Science (26670147, 16H05145, 17 K19534, and 19H03439), and TAKEDA Science Foundation (2015148418) to T.N. and by the Japan Society for the Promotion of Science (16 K15749 and 18H02960) to K.N. R.P.M. was supported by NIH grants HL53325 and HL105314. **Author contributions:** T.N. conceived, designed, and oversaw the experiments. K.N., K.K., T.M., M.H., T.O.A., T.T., H.T., K.T., Y.O., R.P.M., M.T., M.Y., and T.N. performed experiments and analyzed the data. K.N. and T.N. wrote the manuscript. R.P.M. provided critical review on the manuscript. **Competing interests:** The authors declare that they have no competing interests. **Data and materials availability:** All data needed to evaluate the conclusions in the paper are present in the paper and/or the Supplementary Materials. Additional data related to this paper may be requested from the authors.

Submitted 8 April 2020
Accepted 9 October 2020
Published 25 November 2020
10.1126/sciadv.abc1404

Citation: K. Noda, K. Kitagawa, T. Miki, M. Horiguchi, T. O. Akama, T. Taniguchi, H. Taniguchi, K. Takahashi, Y. Ogra, R. P. Mecham, M. Terajima, M. Yamauchi, T. Nakamura, A matricellular protein fibulin-4 is essential for the activation of lysyl oxidase. *Sci. Adv.* **6**, eabc1404 (2020).